Proceedings of the 17th World Congress
The International Federation of Automatic Control
Seoul, Korea, July 6-11, 2008

Positioning of Large-Scale High-Precision Stage with Vibration Suppression PTC

Koichi Sakata * **Hiroshi Fujimoto** * **Kazuaki Saiki** **

* *Yokohama National University, 79-5, Tokiwadai, Hodogaya-ku, Yokohama, 240-8501 Japan (Tel: +81-45-339-4262; e-mail: sakata@hfl.dnj.ynu.ac.jp, hfuji@ynu.ac.jp).*
** *Nikon Corporation, 471, Nagaodai-cho, Sakae-ku, Yokohama, 244-8533 Japan (Tel: +81-45-852-2111; e-mail: saiki.kazu@nikon.co.jp)*

Abstract: In the positioning system of the large-scale high-precision stage, the primary resonance mode appears in low frequency even in the high stiffness stage. The resonance mode is a major obstacle of fast and precise positioning. In this paper, we apply vibration suppression PTC (Perfect Tracking Control) which can control the resonance mode actively on the large-scale stage. Finally, simulations and experiments are performed to show the advantages of the vibration suppression PTC.

1. INTRODUCTION

The large-scale high-precision stage is used in industrial fields such as manufacturing of semiconductors and liquid crystal panels (or displays). Fast and precise positioning control is very important technology related to the improvement of throughput and product quality.

However, the large-scale stage has a low resonance mode because of its structure. It is called that the resonance mode is an obstruction of fast and precise positioning by Otsuka [1995].

Fujimoto et al. [2006] proposed the vibration suppression perfect tracking control (PTC) which can control resonance mode actively in the short-span seeking control of hard disk drives (HDDs). However, the vibration suppression PTC track not "real position" but "virtual position".

In this paper, the vibration suppression PTC is improved to track "real position". Then, the severe specification of positioning of the large-scale high-precision stage is achieved by the vibration suppression PTC. The target specification is the tracking error tolerance 0.5 μm in the positional settling time 150 ms for the large-scale stage with moving part 266 kg.

2. PERFECT TRACKING CONTROL

Fujimoto et al. [2001] proposed the perfect tracking control (PTC) which consists of the 2-DOF control system as shown in Fig .1. This system has two samplers for the reference signal $r(t)$ and the output $y(t)$, and one holder for the input $u(t)$. Therefore, there exist sampling periods T_r, T_y, and T_u which represent the periods of $r(t)$, $y(t)$, and $u(t)$, respectively. PTC applies the multirate feedforward control in which the control input $u(t)$ is changed n times during one sampling period T_r of reference input $r(t)$ as shown in Fig. 2. Here, n is the plant order. H_M in Fig. 1 is the multirate holder which outputs the input

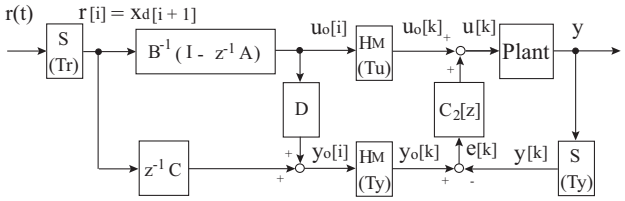

Fig. 1. Perfect tracking control system.

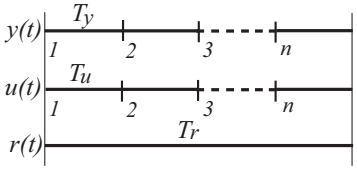

Fig. 2. Multirate sampling period.

$u[i] = [u_1[k] \cdots u_n[k]]^T$ (generated by the long sampling period T_r) on the short sampling period T_u.

Here, the matrices $\boldsymbol{A}$, $\boldsymbol{B}$, $\boldsymbol{C}$, and $\boldsymbol{D}$ of the plant discretized by the long sampling period T_r can be derived as (2) from the plant model discretized by the short sampling period T_u (1).

$$\boldsymbol{x}[k+1] = \boldsymbol{A}_s\boldsymbol{x}[k] + \boldsymbol{b}_s u[k] \ , \ y[k] = \boldsymbol{c}_s\boldsymbol{x}[k] \tag{1}$$

$$\left[\begin{array}{c|c} \boldsymbol{A} & \boldsymbol{B} \\ \hline \boldsymbol{C} & \boldsymbol{D} \end{array}\right] = \left[\begin{array}{c|ccc} \boldsymbol{A}_s^n & \boldsymbol{A}_s^{n-1}\boldsymbol{b}_s & \cdots & \boldsymbol{A}_s\boldsymbol{b}_s \ \ \boldsymbol{b}_s \\ \hline \boldsymbol{c}_s & 0 & \cdots & 0 \ \ 0 \\ \boldsymbol{c}_s\boldsymbol{A}_s & \boldsymbol{c}_s\boldsymbol{b}_s & \cdots & 0 \ \ 0 \\ \vdots & \vdots & \ddots & \vdots \ \ \vdots \\ \boldsymbol{c}_s\boldsymbol{A}_s^{n-1} & \boldsymbol{c}_s\boldsymbol{A}_s^{n-2}\boldsymbol{b}_s & \cdots & \boldsymbol{c}_s\boldsymbol{b}_s \ \ 0 \end{array}\right] \tag{2}$$

Since the matrix $\boldsymbol{B}$ of (2) is non-singular in the case of controllable plant. PTC can be designed as

$$\begin{aligned} \boldsymbol{u}_0[i] &= \boldsymbol{B}^{-1}(\boldsymbol{I} - z^{-1}\boldsymbol{A})\boldsymbol{x}_d[i+1] \\ &= \left[\begin{array}{c|c} \boldsymbol{0} & \boldsymbol{I} \\ \hline -\boldsymbol{B}^{-1}\boldsymbol{A} & \boldsymbol{B}^{-1} \end{array}\right] \boldsymbol{x}_d[i+1] \end{aligned} \tag{3}$$

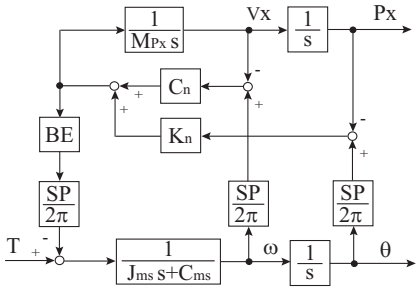

Fig. 3. Model of plant.

$$y_0[i] = z^{-1}\boldsymbol{C}\boldsymbol{x}[i+1] + \boldsymbol{D}\boldsymbol{u}_0[i]. \tag{4}$$

(3) is the stable inverse system of plant as the previewed desired trajectories are given to the state variables of the plant. Therefore, the perfect tracking is assured on the sampling period T_r .

The feedback control $C_2[z]$ suppresses the error between the output $y[k]$ and the nominal output $y_0[k]$ to assure robustness only when disturbances or plant variations exist.

3. MODELING OF STEP-STAGE

X-Y stage which is actuated by ball screw is considerd. X axis of the stage is regarded as the two-inertia system structured by the rotational system of the motor and the translational system of the stage as Fig. 3. X axis is only described in this paper because Y axis can be treated in the same way as X axis. J_{ms} and C_{ms} are inertia and viscosity of motor screw. K_n and C_n are stiffness and viscosity of screw nut. BE is transfer constant from the translational system to the rotational system. The mass of moving part of X axis stage M_{px} is 266 kg. The ball screw pitch SP is 0.01 m/rev. T is the motor torque. P_x and v_x are translational position and translational velocity. θ and ω are rotational position and rotational velocity.

The plant models from motor torque T to translational position P_x and to rotational position θ are represented by (5) and (6). Here, the denominatior of (6) is represented to be equal to that of (5) for the following explanation. The measured frequency responses are shown in Fig. 4. The resonance mode exists at about 70 Hz in low frequency.

$$P(s) = \frac{P_x}{T} = \frac{y}{u} = \frac{b_1 s + b_0}{a_4 s^4 + a_3 s^3 + a_2 s^2 + a_1 s} \tag{5}$$

$$P_\omega(s) = \frac{\omega}{T} = \frac{\omega}{u} = \frac{b_{\omega 3} s^3 + b_{\omega 2} s^2 + b_{\omega 1} s}{a_4 s^4 + a_3 s^3 + a_2 s^2 + a_1 s} \tag{6}$$

$$\begin{cases} a_4 = (2\pi)^2 J_{ms} M_{Px} \\ a_3 = (2\pi)^2 (J_{ms} C_n + M_{Px} C_{ms}) + BE \cdot SP^2 M_{Px} C_n \\ a_2 = (2\pi)^2 (J_{ms} K_n + C_{ms} C_n) + BE \cdot SP^2 M_{Px} K_n \\ a_1 = (2\pi)^2 C_{ms} K_n \\ b_1 = 2\pi \cdot SP \cdot C_n,\ b_0 = 2\pi \cdot SP \cdot K_n \\ b_{\omega 3} = (2\pi)^2 M_{Px},\ b_{\omega 2} = (2\pi)^2 C_n,\ b_{\omega 1} = (2\pi)^2 K_n \end{cases}$$

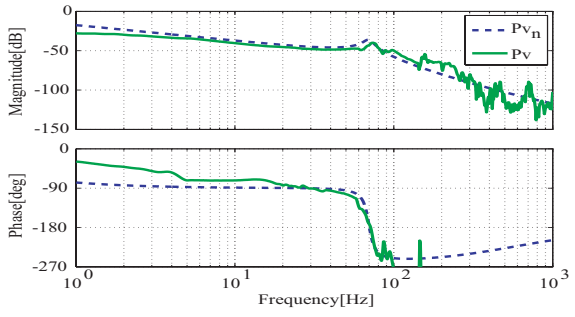

(a) v_x/T

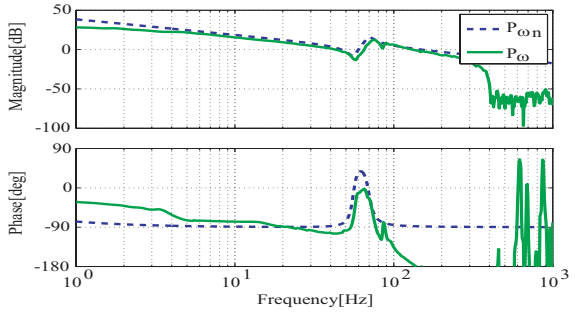

(b) ω/T

Fig. 4. Frequency responses of plant.

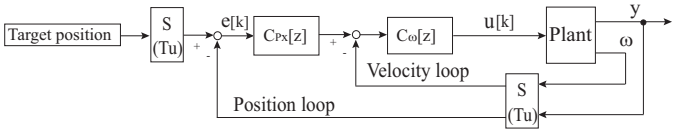

Fig. 5. Feedback Control system.

4. CONTROL SYSTEM DESIGN

4.1 Feedback Controller Design

The conventional control system consists of the feedback controllers based on the translational position controller $C_{Px}(s)$ and the rotational velocity controller $C_\omega(s)$ like Fig. 5. $C_{Px}(s)$ is designed as a proportional controller with a low-pass filter (LPF), and $C_\omega(s)$ is designed as a proportional-integral controller with a phase-lead-compensator. The designed $C_{Px}(s)$ and $C_\omega(s)$ are discretized by Tustin transformation so that the discrete controller $C_{Px}[z]$ and $C_\omega[z]$ are obtained.

Each parameter of the feedback controllers is selected by fine-tuning from frequency responses of the actual experiment. Fig. 6 (a) indicates the frequency response of the rotational velocity feedback loop (from ω_{ref} to ω), and Fig. 6 (b) indicates the frequency response of the entire feedback loop (from y_{ref} to y). It is shown that the bandwidth is about only 3 Hz in Fig. 6 (b). Therefore, The target specification cannot be satisfied only with the feedback controller.

4.2 Singlerate Vibration Suppression PTC

First, PTC is designed in continuous time for two-inertia system model including the resonance mode. An inverse system of the plant P can be represented by

$$u_0 = N(s)\left(a_4 y_0^{(4)} + a_3 y_0^{(3)} + a_2 y_0^{(2)} + a_1 y_0^{(1)}\right), \tag{7}$$

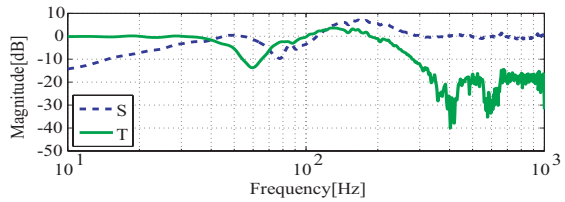

(a) Velocity loop (ω/ω_{ref})

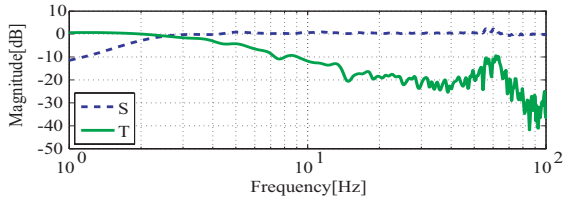

(b) Position loop + Velocity loop (y/y_{ref})

Fig. 6. Frequency responses of S, T.

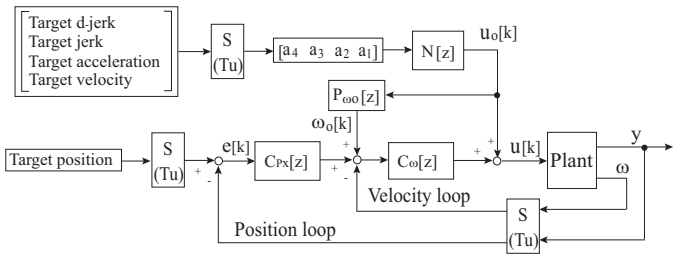

Fig. 7. Singlerate vibration suppression PTC system (proposed method 1).

$$N(s) = \frac{1}{b_1 s + b_0}, \tag{8}$$

from (5). The feedforward input $u_0[k]$ can be given by the desired position trajectory $y_0(t)$. Here, $x^{(n)}$ is n order derivative of x. When the feedforward controller is implemented, $N(s)$ is discretized by Tustin transformation so that the discrete controller $N[z]$ is obtained.

Next, the nominal rotational velocity ω_0 is generated to be compared with the rotational velocity ω in the rotational velocity loop. The rotational plant model of (6) from input u to rotational velocity ω is discretized by zero-order hold so that the discrete rotational plant model $P_\omega[z]$ is obtained. The nominal rotational velocity ω_0 is represented by

$$\omega_0[k] = P_{\omega o}[z] u_0[k]. \tag{9}$$

The singlerate vibration suppression PTC system is shown in Fig. 7. The system can be structure as references are fourth derivatives of the target position as shown in Fig. 7.

Here, note that the discretization error occurs because of a digital re-design of the feedforward controller $N[z]$ in singlerate vibration suppression PTC. Moreover, Åström et al. [1984] indicate that the inverse system of the plant cannot be designed in discrete-time because unstable zero appears in the plant discretized by zero-order hold.

4.3 Multirate Vibration Suppression PTC

The inverse system of the plant cannot be designed in the singlerate control system as explained in the above section. Then, we consider that PTC for two-inertia system model including the resonance mode in the multirate control system explained in Chaper 2. The controllable canonical form of (5) with state variables $\boldsymbol{x} = [z \;\; z^{(1)} \;\; z^{(2)} \;\; z^{(3)}]^T$ is represented by (11) and (12). z is called "virtual position" by Fujimoto et al. [2006].

$$\frac{z}{u} = \frac{b_0}{a_4 s^4 + a_3 s^3 + a_2 s^2 + a_1 s} \tag{10}$$

$$\dot{\boldsymbol{x}}(t) = \boldsymbol{A}_c \boldsymbol{x}(t) + \boldsymbol{b}_c u(t) \;,\; y(t) = \boldsymbol{c}_c \boldsymbol{x}(t) \tag{11}$$

$$\left[\begin{array}{c|c} \boldsymbol{A}_c & \boldsymbol{b}_c \\ \hline \boldsymbol{c}_c & 0 \end{array}\right] = \left[\begin{array}{cccc|c} 0 & 1 & 0 & 0 & 0 \\ 0 & 0 & 1 & 0 & 0 \\ 0 & 0 & 0 & 1 & 0 \\ 0 & -\frac{a_1}{a_4} & -\frac{a_2}{a_4} & -\frac{a_3}{a_4} & \frac{b_0}{a_4} \\ \hline 1 & \frac{b_1}{b_0} & 0 & 0 & 0 \end{array}\right] \tag{12}$$

The discrete-time state equation (1) with zero-order hold is discretized with the sampling period T_u. Here, each sampling period is defined as $T_u = T_y = T_r/4$. Therefore, the multirate feedforward controller is obtained by (2).

The previewed desired trajectories are given to all state variables $\boldsymbol{x}_d = [z_d \;\; z_d^{(1)} \;\; z_d^{(2)} \;\; z_d^{(3)}]^T$. However, the state variables cannot be given directly as references because the virtual position z is not the real position y. The state variable $\boldsymbol{x}_d(t)$ is obtained from the target trajectory $\boldsymbol{r}_d(t) = [y_d \;\; y_d^{(1)} \;\; y_d^{(2)} \;\; y_d^{(3)}]^T(t)$. The transfer function from the translational position P_x to the state variable z is represented as

$$\frac{z}{y} = \frac{b_0}{b_1 s + b_0}, \tag{13}$$

from (5) and (10). Therefore, z_d can be obtained from y_d by inserting the LPF before the input of the references. The LPF is discretized by Tustin transformation in the case that the sampling period T_r is much shorter than the time constant of the LPF. On the other hand, the convolution of time function of the target trajectoy and time function of the LPF is calculated by off-line and it is saved in the memory table in the case that the discretization error is caused.

Moreover, to generate the nominal rotational velocity ω_0, the rotational plant model P_ω of (6) does not need to be inserted in multirate vibration suppression PTC. The state equation of (6) coincides with (12) if matrix $\boldsymbol{c}_c$ is only changed as

$$\boldsymbol{c}_c' = \left[\begin{array}{cccc} 0 & \frac{b_{\omega 1}}{b_0} & \frac{b_{\omega 2}}{b_0} & \frac{b_{\omega 3}}{b_0} \end{array}\right]. \tag{14}$$

It only has to design the matrices $\boldsymbol{C}$ and $\boldsymbol{D}$ of (2) to generate the nominal rotational velocity ω_0. These are defined as $\boldsymbol{C}'$ and $\boldsymbol{D}'$.

Therefore, the multirate vibration suppression PTC can be designed as shown in Fig. 8. Sakata and Fujimoto [2007] proposed the PTC system with cascade feedback for a servo motor. Note that the feedback controllers work only when errors between the nominal output and the actual output are caused by disturbances or modeling errors.

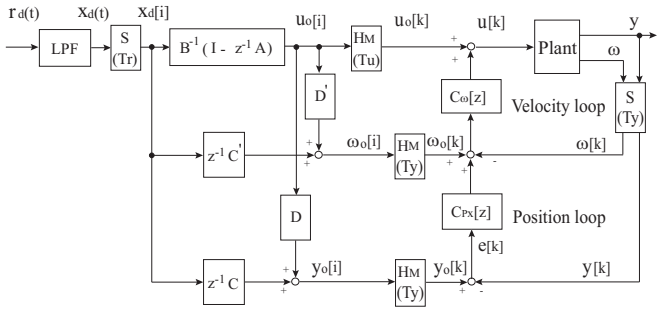

Fig. 8. Multirate vibration suppression PTC system (proposed method 2).

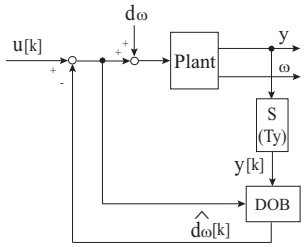

Fig. 9. Plant with disturbance observer.

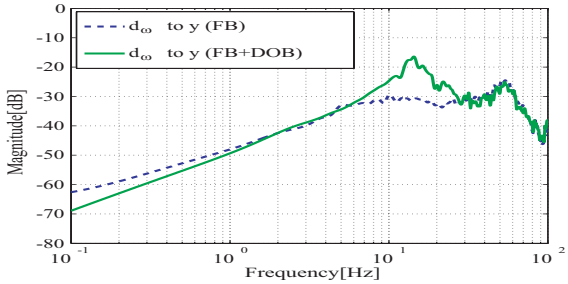

Fig. 10. Frequency responses of disturbance suppression.

4.4 Disturbance Observer Design

The input disturbance by the nonlinear friction of the ball screw is regarded as step-type disturbace. The full-order state observer is designed in discrete-time to estimate and to suppress the disturbance. The discrete state equation of the augmented plant is represented by

$$\boldsymbol{x}_e[k+1] = \boldsymbol{A}_f \boldsymbol{x}_e[k] + \boldsymbol{b}_f u[k] \ , \ y[k] = \boldsymbol{c}_f \boldsymbol{x}_e[k], \quad (15)$$

with the state variables $\boldsymbol{x}_e = [\omega \ \ \theta \ \ v_x \ \ P_x \ \ d_\omega]^T$ added input disturbance d_ω. The full-order state observer can be designed as

$$\hat{\boldsymbol{x}}_e[k+1] = (\boldsymbol{A}_f - \boldsymbol{H}_f \boldsymbol{c}_f)\hat{\boldsymbol{x}}_e[k] + \boldsymbol{b}_f u[k] + \boldsymbol{H}_f y[k] \quad (16)$$

$$\hat{\boldsymbol{x}}_e[k] = [\hat{\omega}[k] \ \ \hat{\theta}[k] \ \ \hat{v}_x[k] \ \ \hat{P}_x[k] \ \ \hat{d}_\omega[k]]^T. \quad (17)$$

The observer gain $\boldsymbol{H}_{ed}$ is designed so that observer poles are located at 100 Hz. Here, estimated disturbance $\hat{d}_\omega$ is subtracted from input u to suppress the disturbance d_ω as shown in Fig. 9. The frequency responses of the disturbance suppression are shown in Fig. 10. The disturbance suppression is improved in the low frequency band below 1 Hz by the disturbance observer.

Table 1. Specifications of target trajectory.

A^{ref}	t_{acc}	t_{con}	t_{dec}	t_d
0.1 m	0.25 s	0.0 s	0.25 s	0.5 s

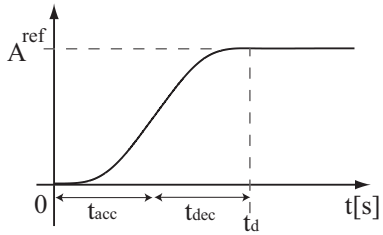

Fig. 11. Target positional trajectory.

5. SIMULATION AND EXPERIMENT

5.1 Simulation

The tracking responses of the feedforward controller of each control system are compared in the case that the plant model is nominal. Each sampling period is $T_u = T_y = T_r/4 = 1/6$ ms. The target position trajectory was generated by sixth-order polynomial equation. The specification of the target position trajectory is shown in Table 1, where the target position is A^{ref}, the acceleration time is t_{acc}, the constant velocity time is t_{con}, the decelerating time is t_{dec}, and the positioning time is t_d ($= t_{acc} + t_{con} + t_{dec}$). The specification is sped up to limit of ball screw. The target positional trajectory is shown in Fig. 11. The target velocity and acceleration and jerk trajectories are given by differentiating the target position trajectory.

The target specification is the tracking error tolerance 0.5 μm in the positional settling time 150 ms. Here, the positional settling time is the time in which the tracking error converges in the tolerance after the positioning time t_d.

The nominal simulation results of the comparison only with the feedforward controller are shown in Fig. 12. After 0.5 s, the tracking error of the singlerate vibration suppression PTC is over 0.5 μm by the influence of the discretization error of the feedforward controller. On the other hand, the tracking error of the multirate vibration suppression PTC is perfectly zero at sampling points.

5.2 Experiment

The tracking response of each control system is compared in the actual experiment. The sampling periods and the target trajectories are same with those of the simulation. Moreover, the disturbance observer is implemented in the experiment. The experimantal results are shown in Fig. 13. The tracking errors of five time experiments are overwritten for the confirmation of reproducibility. The tracking error tolerance 0.5 μm was achieved over the positional settling time 200 ms in the singlerate vibration suppression PTC. On the other hand, the tracking error tolerance 0.5 μm was achieved in the positional settling time 15 ms in the multirate vibration suppression PTC.

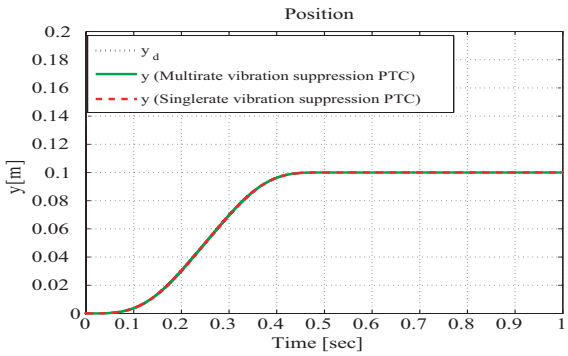

(a) Position response

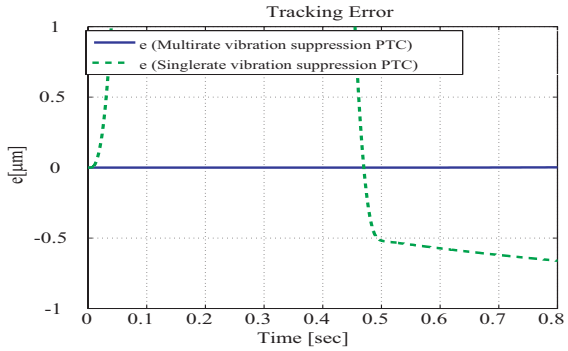

(b) Tracking error

Fig. 12. Nominal simulation results (only with feedforward controller).

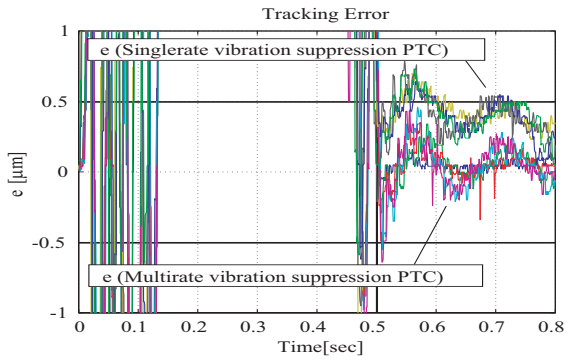

Fig. 13. Experimental results.

6. IMPROVEMENT OF FEEDBACK CONTROLLER

The conventional feedback system was designed by the traditional double loop controller with fine-tuning. Because it is not very theoretical and systematic, the feedback performance has to depend on tuning of engineers. Then, a feedback controller which consists of the observer and the regulator is applied to improve the feedback system.

In order to regulate the plant state and reject the disturbance, the regulator is designed by

$$u[k] = \boldsymbol{F}\hat{\boldsymbol{x}}_e[k] = \boldsymbol{F}_p\hat{\boldsymbol{x}}_p[k] + F_d\hat{x}_d[k], \tag{18}$$

where $\hat{\boldsymbol{x}}_p[k] = [\hat{\omega}[k] \;\; \hat{\theta}[k] \;\; \hat{v}_x[k] \;\; \hat{P}_x[k]]$, $\hat{x}_d[k] = \hat{d}_\omega[k]$ and $\boldsymbol{F} = [\boldsymbol{F}_p \;\; F_d]$. The feedback type controller which consists of the observer and the regulator is obtained by

$$u[k] = \left[\begin{array}{c|c} \boldsymbol{A}_f - \boldsymbol{H}_f\boldsymbol{c}_f + \boldsymbol{b}_f\boldsymbol{F} & \boldsymbol{H}_f \\ \hline \boldsymbol{F} & 0 \end{array}\right] y[k], \tag{19}$$

with (17) and (18). Therefore, the feedback controller can be applied in PTC system shown in Fig. 1 as

$$\begin{aligned} u[k] &= C_2[z](y_o[k] - y[k]) \\ &= C_2[z]e[k] \\ &= \left[\begin{array}{c|c} \boldsymbol{A}_f - \boldsymbol{H}_f\boldsymbol{c}_f + \boldsymbol{b}_f\boldsymbol{F} & -\boldsymbol{H}_f \\ \hline \boldsymbol{F} & 0 \end{array}\right] e[k]. \end{aligned} \tag{20}$$

The feedback controller can be designed systematically in comparison with the conventional feedback controller.

Frequency responses of one design example are shown in Fig. 14 and 15. The observer and the regulator are designed by pole placement to suppress the resonance mode of the plant. Figures show that the bandwidth and the disturbance suppression performance are extremely improved in comparison with the conventional feedback controller because the proposed controller is designed with considering resonance mode of the plant clearly.

The experimental results of the time responses of the conventional feedback and the proposed feedback are shown in Fig. 16. The target trajectory is the same as simulation in Table 1. In the experiment of Fig. 13, the multirate feedforward controller is sufficiently adjusted. In the experiment of Fig. 16, the multirate feedforward controller is however not very adjusted.

The tracking error in the acceleration and deceleration time ($0 \sim 0.5$ sec) is dramatically suppressed in Fig. 16(a) and (c) because of the high bandwidth of the feedback system. However, the positional settling time is not shortened as expected. It seems that the reason for the result is a nonlinear characteristic of the ball screw. The group of balls rolls over linearly in the acceleration and deceleration time. The group of balls acts as a non-linear spring in the positional settling time because this does not roll over clearly. Therefore, if the high bandwidth of the feedback system is achieved, the feedback performance is not always brought out in the positional settling time.

In this paper, it is regarded that the feedback controllers suppress variation of viscosity and nonlinear friction caused by the ball screw. Iwasaki et al. [2006] proposed a modeling of the nonlinear friction. Higher precise positioning can be expected by the feedforward compensation of the nonlinear friction.

7. CONCLUSION

Vibration suppression PTC was applied to fast and precise positioning of the large-scale high-precision stage which has low resonance mode. The target specification of the large-scale stage with the moving part 266 kg is tracking error tolerance 0.5 μm in the positional settling time 150 ms. It was achieved against the target trajectory sped up to limit of ball screw in simulations and experiments. Especially, the multirate vibration suppression PTC achieved ten times as good as the target specification in experiments. Moreover, the improvement of feedback controller which can be designed systematically was shown. The transient of the positioning is dramatically improved by the feedback controller.

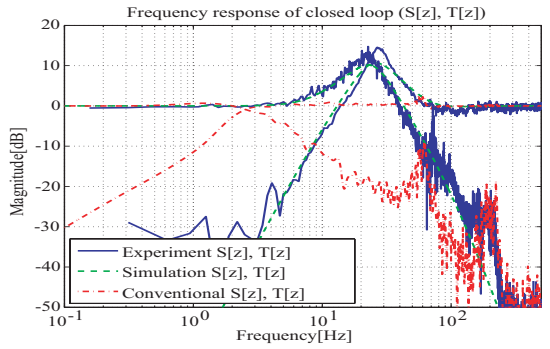

(a) Closed loop

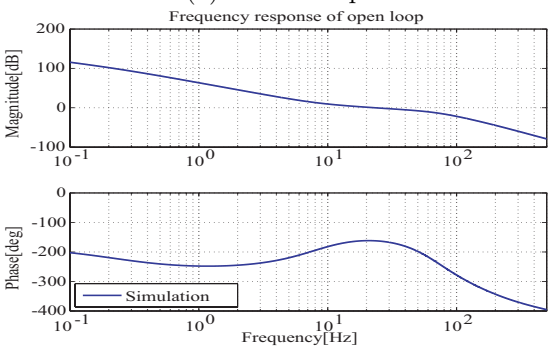

(b) Open loop

Fig. 14. Frequency responses (Improvement).

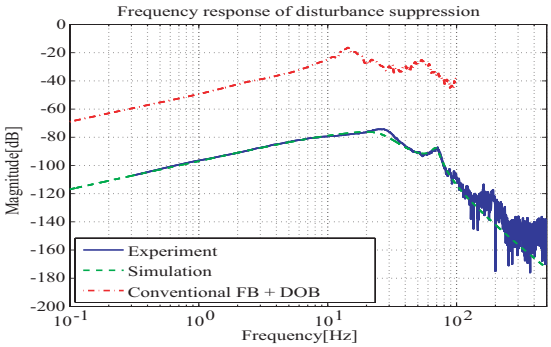

Fig. 15. Frequency response of disturbance suppression (Improvement).

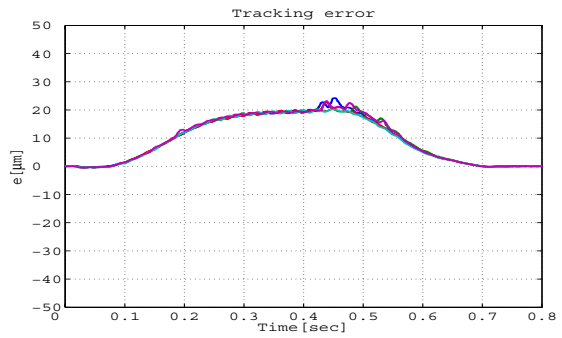

(a) Conventional FB

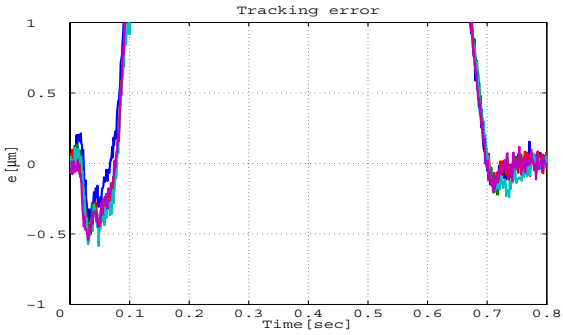

(b) Conventional FB (expanded)

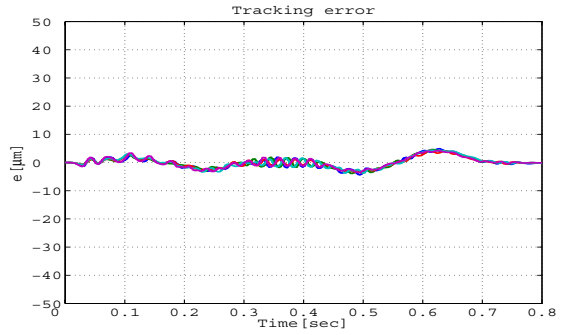

(c) Proposed FB

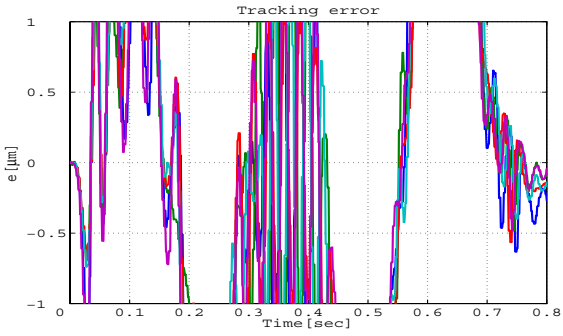

(d) Proposed FB (expanded)

Fig. 16. Time response.

REFERENCES

J. Otsuka. Present and Future Technique of Ultraprecision Positioning. *JSPE*, vol. 61, no. 12, pp. 1645–1649, 1995 (in Japanese).

H. Fujimoto, K. Fukushima and S. Nakagawa. Vibration suppression short-span seeking of HDD with multirate feedforward control. in *Proc. American Control Conference*, Minneapolis, June, 2006.

H. Fujimoto, Y. Hori and A. Kawamura. Perfect Tracking Control based on Multirate Feedforward Control with Generalized Sampling Periods. *IEEE Trans. Industrial Electronics*, vol. 48, no. 3, pp. 636–644, 2001.

K. J. Åström, P. Hangander and J. Sternby. Zeros of sampled system. *Automatica*, vol. 20, no. 1, pp. 31–38, 1984.

K. Sakata and H. Fujimoto. Perfect Tracking Control of Servo Motor Based on Precise Model with PWM Hold and Current Loop. in *Proc. The Fourth Power Conversion Conference*, pp. 1612–1617, Nagoya, 2007.

M. Iwasaki, M. Kawafuku and H. Hirai. 2DOF Control-Based Fast and Precise Positioning for Vibratory Mechanism with Nonlinear Friction. in *Proc. IEEE International Conference on Mechatronics*, pp. 27–31, 2006.